

# Climate change in cities due to global warming and urban effects

Mark P. McCarthy,<sup>1</sup> Martin J. Best,<sup>2</sup> and Richard A. Betts<sup>1</sup>

Received 24 February 2010; revised 1 April 2010; accepted 6 April 2010; published 8 May 2010.

[1] Urbanisation is estimated to result in 6 billion urban dwellers by 2050. Cities will be exposed to climate change from greenhouse gas induced radiative forcing, and localised effects from urbanisation such as the urban heat island. An urban land-surface model has been included in the HadAM3 Global Climate Model. It shows that regions of high population growth coincide with regions of high urban heat island potential, most notably in the Middle East, the Indian sub-continent, and East Africa. Climate change has the capacity to modify the climatic potential for urban heat islands, with increases of 30% in some locations, but a global average reduction of 6%. Warming and extreme heat events due to urbanisation and increased energy consumption are simulated to be as large as the impact of doubled CO<sub>2</sub> in some regions, and climate change increases the disparity in extreme hot nights between rural and urban areas. **Citation:** McCarthy, M. P., M. J. Best, and R. A. Betts (2010), Climate change in cities due to global warming and urban effects, *Geophys. Res. Lett.*, 37, L09705, doi:10.1029/2010GL042845.

## 1. Introduction

[2] Urban micro-climates have long been recognised [Howard, 1833; Oke, 1987], and in the monitoring and detection of global climate change climatologists have gone to great lengths to remove or minimise the potential influence of urbanisation on the historical climate record [Parker, 2010]. This is vital for trying to detect warming trends of the order 0.1°C per decade. However, observational evidence shows trends in urban heat islands in some locations of a similar magnitude or greater than that from greenhouse gas forced climate change [Stone, 2007; Fujibe, 2009] and further urbanisation of the global population is expected through the 21st century [United Nations, 2007]. The latest report from the Intergovernmental Panel on Climate Change recognises that urbanisation is missing from climate model projections [Christensen et al., 2007], and the potential for differential rates of radiatively-forced climate change in urban compared to rural areas has received little attention.

[3] The magnitude of the urban heat island is a function of urban morphology and physical characteristics, urban extent, waste heat release, and regional climate factors [see, e.g., Oke, 1987; Arnfield, 2003; Kanda, 2007]. Advances in recent decades have produced a variety of numerical models designed to simulate the key processes governing heat, moisture and momentum exchanges of the urban canopy [Grimmond et al., 2010]. Recent analysis by Oleson et al.

[2010] use an urban scheme within a Global Climate Model (GCM) to quantify the potential impact of white roofs as a climate mitigation strategy. In this paper we use an urban land surface scheme coupled to a GCM as an integrated method to quantify the impact of large-scale and local drivers of climate change on the urban environment, and demonstrate that these effects should not be treated independently when making projections of urban climate change.

## 2. Method

[4] We have included capability for sub-grid scale variations in surface properties, allowing multiple land surface types to occupy each GCM grid cell [Essery et al., 2003], and an urban land-surface scheme [Best et al., 2006] within the Hadley Centre Global Climate Model (HadAM3) [Pope et al., 2000]. The urban surface scheme simulates a canopy layer with urban thermal properties, radiatively coupled to the underlying soil scheme, controlling exchanges of heat, water, and momentum at the atmosphere-surface interface. The methods are described in more detail in the auxiliary material and evaluated by Best et al. [2006].<sup>3</sup>

[5] Urban areas are the major source of carbon dioxide emissions contributing to greenhouse gas forced climate change [Grimmond, 2007]. The associated waste heat released to the environment in cities is a well documented driver of urban micro-climates. Averaged globally anthropogenic waste heat is of order 0.03 Wm<sup>-2</sup>, and has generally been ignored as a climate forcing [Flanner, 2009]. However, in cities waste heat resulting from heating and cooling of buildings, traffic, and even human metabolism is a significant contribution to the surface energy budget. Estimates of the magnitude of this heat source range from tens to hundreds of Wm<sup>-2</sup> in U.S. and European cities [Sailor and Lu, 2004; Pigeon et al., 2007] and as high as 1590 Wm<sup>-2</sup> for the business district of Tokyo [Ichinose et al., 1999]. A set of simulations have been conducted with an anthropogenic heating term added directly to the surface energy balance equation of the urban canopy model.

[6] Urban coverage is defined in the model by the DIS-Cover dataset [Loveland et al., 2000] which has a global urban coverage of 271,956 km<sup>2</sup>. Experiments were conducted with two scenarios of urban energy use. The first uses 20 Wm<sup>-2</sup> or an additional 169 × 10<sup>18</sup> J of energy globally, which is 50% of the estimated 335 × 10<sup>18</sup> J global energy demand in cities in 2006 [International Energy Agency, 2008]. Urban areas account for only a small fraction of any model grid cell so the choice of land cover data will have minimal impact on the results presented. A second experiment at an elevated heat flux of 60 Wm<sup>-2</sup> yields 506 × 10<sup>18</sup> J which is well within the range of projected consumption by 2100

<sup>1</sup>Met Office Hadley Centre, Fitzroy Road, Exeter, UK.

<sup>2</sup>Joint Centre for Hydro-Meteorological Research, Met Office, Crowmarsh Gifford, UK.

<sup>3</sup>Auxiliary materials are available in the HTML. doi:10.1029/2010GL042845.

**Table 1.** Summary of Model Experiments<sup>a</sup>

Name	CO <sub>2</sub> Mixing Ratio	Urban Land Surface	Anthropogenic Heat Flux
C1U	323ppm	Y	N
C2U	645ppm	Y	N
C1U20	323ppm	Y	20Wm <sup>-2</sup>
C2U20	645ppm	Y	20Wm <sup>-2</sup>
C2U60	645ppm	Y	60Wm <sup>-2</sup>

<sup>a</sup>All experiments were run for 25 years and the first year of simulation excluded from analysis to allow for model spinup.

from the Special Report on Emissions Scenarios (SRES) [Nakićenović and Swart, 2000]. The experiments conducted are not intended to represent formal projections, but are within reasonable bounds of current and future energy projections, and therefore represent plausible values for quantifying sensitivity. The equivalent global forcing from the additional energy input is 0.01Wm<sup>-2</sup> and 0.03Wm<sup>-2</sup> at 20Wm<sup>-2</sup> and 60Wm<sup>-2</sup> respectively.

[7] The set of experiments conducted are outlined in Table 1, with low (323ppm) and high (645ppm) levels of atmospheric CO<sub>2</sub>. The experimental design is to isolate the urban climate response to global and local climate forcings under different regional climate regimes, so we use the same urban properties, and same anthropogenic heat release everywhere. This means we do not quantify the role of different urban surfaces, or the heterogeneity across a city. The urban model has previously been evaluated against Vancouver and Mexico City [Best et al., 2006; Grimmond et al., 2010] and London [Best, 2005] providing evidence that the model does capture bulk properties of the meso-scale near-surface energy exchange and temperature evolution. We define the simulated urban heat island as the near surface air-temperature difference between the urban and dominant non-urban land surface type located within each GCM gridcell. Daily minimum and maximum (Tmin, Tmax) are used as representative of night and day heat islands and treated separately. The global results have been masked to major populated areas in 2050 from the A2 SRES scenario downscaled by van Vuuren et al. [2007] and shown in Figure 1 (top).

### 3. Impact of Atmospheric CO<sub>2</sub> on Urban Heat Island

[8] Large population and urbanisation trends are projected in parts of Africa and Asia (Figure 1, top) [United Nations [2007], which will require considerable growth in the urban land footprint in these areas. Urban areas located in Northern Africa, the Middle East, and Western Asia have nocturnal urban heat islands up to five times larger than the median value of 1°C sampled from all populated regions in experiment C1U (Figure 1, bottom). The largest heat islands are found in sub-tropical arid climates where the diurnal temperature range is large. This results from a combination of high incident short wave radiation at the surface, and low soil moisture, resulting in large energy gain during the day, but low surface heat capacity and rapid cooling rates of the soil or vegetation surface at night, yielding larger nocturnal differences in urban and rural temperature.

[9] The change in the simulated nocturnal heat island in response to 2xCO<sub>2</sub> (C2U-C1U) is in excess of 30% in some locations (Figure 2) such as along parts of the Eastern sea-

board of the U.S., South America, and South East Asia. The change in the global area averaged nocturnal heat island is a modest reduction of 6% ± 1%. The simulated heat islands respond to climate change through those feedbacks, such as cloud or soil moisture, that influence important components of the surface energy balance. The impact on the absolute heat island in these simulations is generally of order a few tenths of a degree, compared to the radiatively forced warming of order 3°C, but it demonstrates that the magnitude of the urban heat island is not static under climate change.

### 4. Impact of Urbanisation on Local Climate Change

[10] The net impact on temperature in HadAM3 in response to the doubling of atmospheric CO<sub>2</sub>, inclusion of an urban surface, and the two rates of anthropogenic heating are summarised in Figure 3. The global mean response in Tmin to doubling of CO<sub>2</sub> in this model is a rise of 3.2°C, and the sub-regions experience warming of between 2.3°C and 3.4°C. Including urban factors increases the total warming to 6.2°C over urban surface in the Middle East due to its high

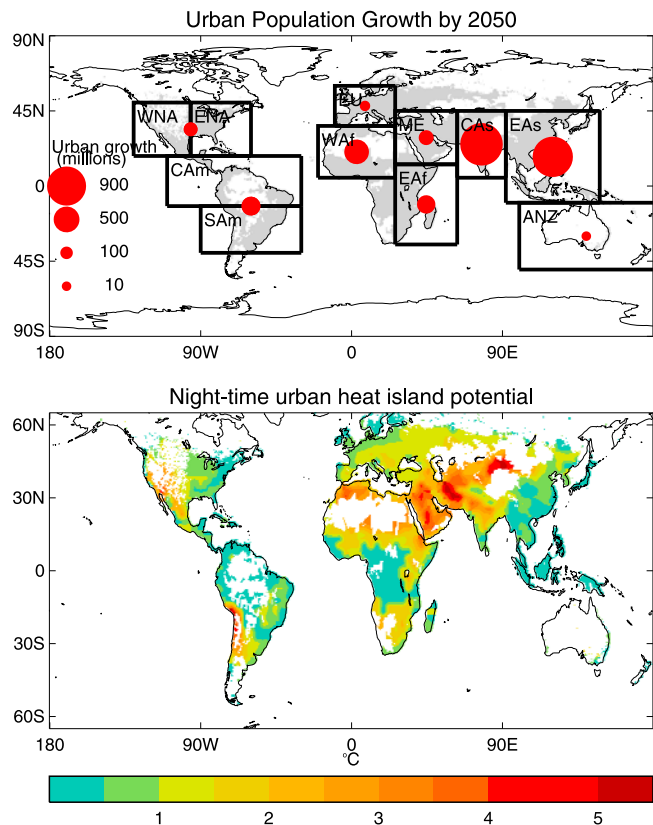


**Figure 1.** Population growth and the urban heat island potential. (top) Estimates of urban population growth between the years 2000 and 2050 [United Nations, 2007] for a number of global regions, and grey shading represents 2050 major populated areas (>10000 people per 0.5° latitude, longitude cell [van Vuuren et al., 2007]). (bottom) Simulated urban heat island as the difference in 24 year mean Tmin between the urban tile temperature and the dominant non-urban tile within each gridcell of experiment C1U (see text and Table 1), and masked to the populated regions defined in the upper panel.

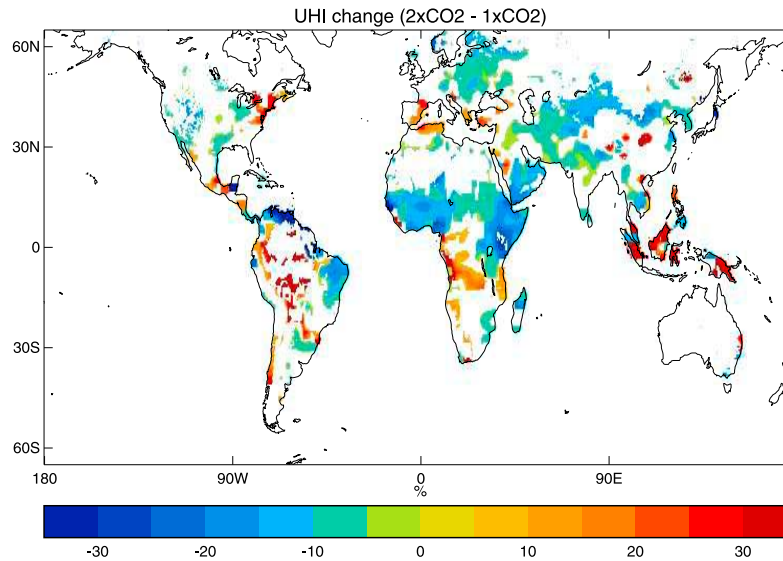


**Figure 2.** Change in urban heat island in response to doubled  $\text{CO}_2$ . UHI difference between experiments C2U and C1U (see text and Table 1) as a percentage of the C1U value. The data have been masked to populated regions of Figure 1 (top), and are only shown where the difference is significant at the 95% level.

potential for nocturnal urban heat islands. The anthropogenic heat release has a similar impact on night temperature in all regions with an average  $0.2^\circ\text{C}$  warming at  $20\text{Wm}^{-2}$  and  $0.6^\circ\text{C}$  at  $60\text{Wm}^{-2}$ . In contrast the warming of  $T_{\text{max}}$  is dominated by climate change (Figure 3b), with urban land inducing  $0.5^\circ\text{C}$  increase, and anthropogenic heat resulting in  $0.1^\circ\text{C}$  and  $0.2^\circ\text{C}$  increase at  $20\text{Wm}^{-2}$  and  $60\text{Wm}^{-2}$  respectively, due to its relatively small magnitude in relation to the daytime solar forcing.

[11] Those regions with the higher cumulative impact of climate change and urban effects (toward the left of Figure 3a) are, with the exception of Western North America (WNA) also projected to at least double their urban population by 2050 (coloured red in Figure 3c based on *United Nations* [2007]). The impacts of anthropogenic climate change on people and infrastructure will be sensitive to these potentially large additional drivers of change due to urbanization, and heat release.

[12] Assessments of the potential health and well-being of populations under a changing climate are often driven by regional or global climate model projections to provide baseline temperature increases, in conjunction with mortality-climate statistics that are often drawn from urban populations [Confalonieri *et al.*, 2007]. The frequency and occurrence of heatwaves [e.g., Tebaldi *et al.*, 2006] are vital for assessing vulnerabilities and risks to urban populations. The impact of climate and urban effects on extreme events are summarised for the urban surface of GCM grid cells that contain the locations of a number of global cities in Figure 4. The choice of location is illustrative of regional impacts, and these results do not represent formal climate projections for these cities. Hot nights are defined as the frequency that  $T_{\text{min}}$  for rural and urban surfaces exceed the 99th percentile of the  $T_{\text{min}}$  temperature distribution over the local non-urban surface.

[13] Climate change increases hot days by a similar amount for both urban and rural situations (not shown). However, rural and urban increases differ significantly for the frequency of hot nights shown in Figure 4. While Beijing as a rural

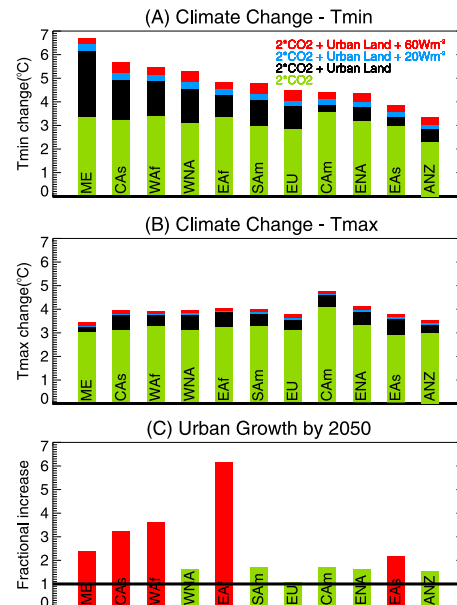


**Figure 3.** Simulated climate change in response to doubled  $\text{CO}_2$  and urban effects for geographical sub-regions. Regions are shown in Figure 1 and represent the Middle East (ME), Central Asia (CAs), West Africa (WAF), West North America (WNA), East Africa (EAF), South America (SAM), Europe (EU), Central America (CAM), East North America (ENA), Australia and New Zealand (ANZ). Shown are the cumulative impact on (a)  $T_{\text{min}}$  and (b)  $T_{\text{max}}$ , relative to the non-urban surface of C1U of doubled  $\text{CO}_2$ , (green, C2U non-urban), the urban heat island (black, C2U urban), the impact of  $20\text{Wm}^{-2}$  anthropogenic heat release (blue, C2U20), and the impact of  $60\text{Wm}^{-2}$  anthropogenic heat release (red, C2U60). (c) The urban population in 2050 as a fraction of the urban population in 2000 [United Nations, 2007]. Regions where the urban population is expected to exceed twice the 2000 level are highlighted in red, and the solid line indicates the line of no change.

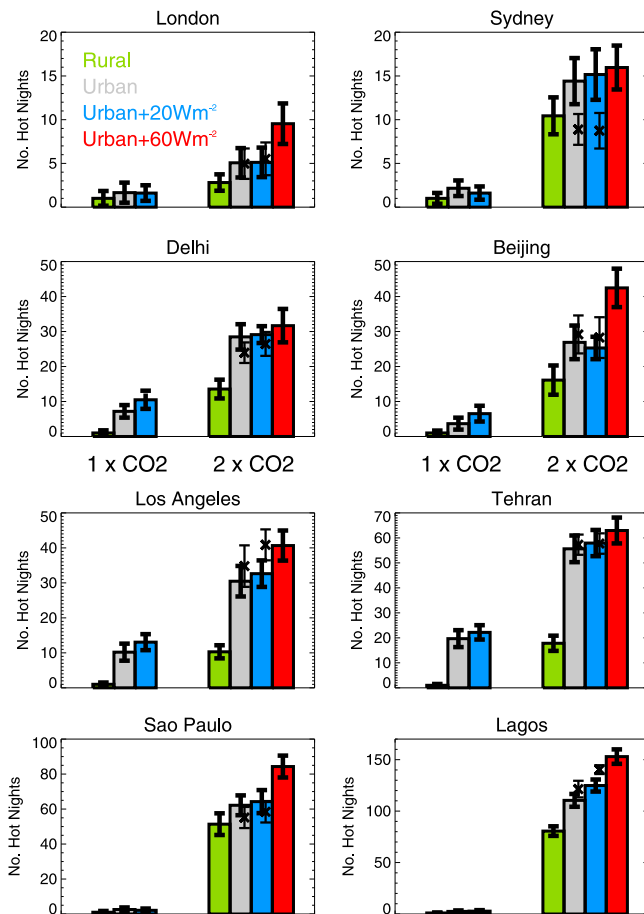


**Figure 4.** Annual frequency of hot nights for global city locations for  $1\times\text{CO}_2$  (C1U) and  $2\times\text{CO}_2$  (C2U, C2U20, C2U60). Bars reflect the average annual frequency that night time minimum temperature exceeds the 99th percentile of the non-urban C1U temperature. Error bars denote the 95% confidence interval around the estimated average, i.e., they only represent statistical sampling uncertainty, they do not represent climate change or other sources of uncertainty. Crosses represent the hot days/nights estimated by applying the radiatively forced climate change from the non-urban temperature to the simulated urban heat island from C1U.

surface has 14 additional hot nights under the  $2\times\text{CO}_2$  experiment, the urban surface has 26 additional hot nights and a further 15 hot nights for the case of  $60\text{Wm}^{-2}$ , resulting in a total of 42 hot nights in Beijing for the future  $60\text{Wm}^{-2}$  climate. In Lagos hot nights in the  $2\times\text{CO}_2$  experiments reach 153 per year for the  $60\text{Wm}^{-2}$  experiment compared to 81 for the rural situation.

[14] Occurrence of hot nights under climate change might also be estimated by applying the radiatively-forced climate change pattern given by C2U to the urban-induced warming in the C1U experiments. In other words assume that the present day urban heat island can be linearly added to a future climate. Such estimates are shown by crosses in Figure 4. The estimate for London and Tehran are similar to those found by the urban-climate model, but for other locations significant differences are apparent with underestimates in Sydney, Delhi, and Sao Paulo, and overestimates for Beijing,

Los Angeles and Lagos. Applying a present day heat island to future climate projections in this way is not adequate for assessing future climate impacts in cities. Furthermore, such a strategy cannot account for changes in the anthropogenic heat release that have a large impact on the occurrence of hot nights. The inclusion of  $60\text{Wm}^{-2}$  can result in a significant increase in extreme hot nights in the case of London and Beijing of a similar impact as doubling of  $\text{CO}_2$ . Climate change results in a greater increase of hot nights for cities than neighbouring rural areas, increasing the thermal stress and vulnerability to heat waves of urban-citizens in a warmer climate compared to their rural counterparts.

[15] The results of these simulations demonstrate the potential exposure of urban populations to climate change and how it is enhanced by local factors. For climate impacts and adaptation research it is important to understand and estimate risks of future climate stress, so it is essential to account not only for climate change, but also population dynamics, urbanisation and energy use. The continued development of urban land-surface schemes suitable for climate models will greatly assist in further developing our understanding of climate change in cities [Best, 2005; Masson, 2006; Oleson *et al.*, 2008]. GCMs can provide a powerful tool for quantifying the potential cumulative impacts of climate change for urban society and infrastructure as a result of both global and local climate forcings.

[16] **Acknowledgments.** This work was supported by the Joint DECC and Defra Integrated Climate Programme - DECC/Defra (GA01101).

## References

- Arnfield, A. J. (2003), Two decades of urban climate research: A review of turbulence, exchanges of energy and water, and the urban heat island, *Int. J. Climatol.*, 23, 1–26, doi:10.1002/joc.859.
- Best, M. J. (2005), Representing urban areas within operational numerical weather prediction models, *Boundary Layer Meteorol.*, 114, 91–109, doi:10.1007/s10546-004-4834-5.
- Best, M. J., C. S. B. Grimmond, and M. G. Villani (2006), Evaluation of the urban tile in MOSES using surface energy balance observations, *Boundary Layer Meteorol.*, 118, 503–525, doi:10.1007/s10546-005-9025-5.
- Christensen, J. H., et al. (2007), Regional climate projections, in *Climate Change 2007: The Physical Science Basis. Contribution of Working Group I to the Fourth Assessment Report of the Intergovernmental Panel on Climate Change*, edited by S. Solomon *et al.*, pp. 847–940, Cambridge Univ. Press, Cambridge, U. K.
- Confalonieri, U., et al. (2007), Human health, in *Climate Change 2007: Impacts, Adaptation and Vulnerability. Contribution of Working Group II to the Fourth Assessment Report of the Intergovernmental Panel on Climate Change*, edited by M. L. Parry *et al.*, pp. 391–431, Cambridge Univ. Press, Cambridge, U. K.
- Essery, R. L. H., M. J. Best, R. A. Betts, P. M. Cox, and C. M. Taylor (2003), Explicit representation of subgrid heterogeneity in a GCM land-surface scheme, *J. Hydrometeorol.*, 4, 530–543, doi:10.1175/1525-7541(2003)004<0530:EROSH>2.0.CO;2.
- Flanner, M. G. (2009), Integrating anthropogenic heat flux with global climate models, *Geophys. Res. Lett.*, 36, L02801, doi:10.1029/2008GL036465.
- Fujibe, F. (2009), Detection of urban warming in recent temperature trends in Japan, *Int. J. Climatol.*, 29, 1811–1822, doi:10.1002/joc.1822.
- Grimmond, S. (2007), Urbanization and global environmental change: Local effects of urban warming, *Geogr. J.*, 173, 83–88, doi:10.1111/j.1475-4959.2007.232.3.x.
- Grimmond, S., et al. (2010), The International Urban Energy Balance Models Comparison Project: First results from Phase 1, *J. Appl. Meteorol. Climatol.*, doi:10.1175/2010JAMC2354.1, in press.
- Howard, L. (1833), *The Climate of London: Deduced From Meteorological Observations Made in the Metropolis and Various Places Around It*, Harvey and Darton, London.
- Ichinose, T., K. Shimodono, and K. Hanaki (1999), Impact of anthropogenic heat on urban climate in Tokyo, *Atmos. Environ.*, 33, 3897–3909, doi:10.1016/S1352-2310(99)00132-6.

- International Energy Agency (2008), *World Energy Outlook 2008*, Int. Energy Agency, Paris.
- Kanda, M. (2007), Progress in urban meteorology: A review, *J. Meteorol. Soc. Jpn.*, 85B, 363–383, doi:10.2151/jmsj.85B.363.
- Loveland, T. R., B. C. Reed, J. F. Brown, O. Ohlen, Z. Zhu, L. Yang, and J. W. Merchant (2000), Development of a global land cover characteristics database and IGBP DISCover from 1 km AVHRR data, *Int. J. Remote Sens.*, 21, 1303–1330, doi:10.1080/014311600210191.
- Masson, V. (2006), Urban surface modelling and the meso-scale impact of cities, *Theor. Appl. Climatol.*, 84, 35–45, doi:10.1007/s00704-005-0142-3.
- Nakićenović, N., and R. Swart (Eds.) (2000), *Special Report on Emissions Scenarios. A Special Report of Working Group III of the Intergovernmental Panel on Climate Change*, 599 pp., Cambridge Univ. Press, Cambridge, U. K.
- Oke, T. (1987), *Boundary Layer Climates*, 2nd ed., 435 pp., Methuen, London.
- Oleson, K. W., G. B. Bonan, J. Feddema, M. Vertenstein, and C. S. B. Grimmond (2008), An urban parameterization for a global climate model. Part I: Formulation and evaluation for two cities, *J. Appl. Meteorol. Climatol.*, 47, 1038–1060, doi:10.1175/2007JAMC1597.1.
- Oleson, K. W., G. B. Bonan, and J. Feddema (2010), The effects of white roofs on urban temperature in a global climate model, *Geophys. Res. Lett.*, 37, L03701, doi:10.1029/2009GL042194.
- Parker, D. E. (2010), Urban heat island effects on estimates of observed climate change, *Clim. Change*, 1, 123–133, doi:10.1002/wcc.21.
- Pigeon, G., D. Legain, P. Durand, and V. Masson (2007), Anthropogenic heat release in an old European agglomeration (Toulouse, France), *Int. J. Climatol.*, 27, 1969–1981, doi:10.1002/joc.1530.
- Pope, V. D., M. L. Gallani, P. R. Rowntree, and R. A. Stratton (2000), The impact of new physical parametrizations in the Hadley Centre climate model: HadAM3, *Clim. Dyn.*, 16, 123–146, doi:10.1007/s003820050009.
- Sailor, D. J., and L. Lu (2004), A top-down methodology for developing diurnal and seasonal anthropogenic heating profiles for urban areas, *Atmos. Environ.*, 38, 2737–2748, doi:10.1016/j.atmosenv.2004.01.034.
- Stone, B. (2007), Urban and rural temperature trends in proximity to large US cities: 1951–2000, *Int. J. Climatol.*, 27, 1801–1807, doi:10.1002/joc.1555.
- Tebaldi, C., K. Hayhoe, J. M. Arblaster, and G. A. Meehl (2006), Going to the extremes: An intercomparison of model-simulated historical and future changes in extreme events, *Clim. Change*, 79, 185–211, doi:10.1007/s10584-006-9051-4.
- United Nations (2007), *World Urbanization Prospects: The 2007 Revision*, Dep. of Econ. and Soc. Affairs, U. N., New York. (Available at <http://www.un.org/esa/population/publications/wup2007/2007wup.htm>)
- van Vuuren, D. P., et al. (2007), Downscaling drivers of global environmental change: Enabling use of global SRES scenarios at the national and grid levels, *Global Environ. Change*, 17, 114–130.

---

M. J. Best, Joint Centre for Hydro-Meteorological Research, Met Office, Maclean Building, Benson Lane, Crowmarsh Gifford OX10 8BB, UK.  
 R. A. Betts and M. P. McCarthy, Met Office Hadley Centre, Fitzroy Road, Exeter EX1 3PB, UK. (mark.mccarthy@metoffice.gov.uk)